Reference-free deconvolution of complex DNA methylation data – a detailed protocol

Michael Scherer[1,2,3], Petr V. Nazarov[4], Reka Toth[5], Shashwat Sahay[1], Tony Kaoma[4], Valentin Maurer[5], Christoph Plass[5], Thomas Lengauer[3], Jörn Walter[1], and Pavlo Lutsik[5]

[1] Department of Genetics/Epigenetics, Saarland University, 66123 Saarbrücken, Germany
[2] Graduate School of Computer Science, Saarland Informatics Campus, 66123 Saarbrücken, Germany
[3] Research Group Computational Biology, Max Planck Institute for Informatics, 66123 Saarbrücken, Germany
[4] Quantitative Biology Unit, Luxembourg Institute of Health, Luxembourg
[5] Division of Cancer Epigenomics, German Cancer Research Center (DKFZ), 69120 Heidelberg, Germany

Abstract

Epigenomic profiling enables unique insights into human development and diseases. Often the analysis of bulk samples remains the only feasible option for studying complex tissues and organs in large patient cohorts, masking the signatures of important cell populations in convoluted signals. DNA methylomes are highly cell type-specific, enabling recovery of hidden components using advanced computational methods without the need of reference profiles. We propose a three-stage protocol for reference-free deconvolution of DNA methylomes comprising: (i) data preprocessing, confounder adjustment and feature selection, (ii) deconvolution with multiple parameters, and (iii) guided biological inference and validation of deconvolution results. Our protocol simplifies the analysis and integration of DNA methylomes derived from complex tissues, including tumors. Applying this protocol to lung cancer methylomes from TCGA revealed components linked to stromal cells, tumor-infiltrating immune cells, and associations with clinical parameters. The protocol takes less than four days to complete and requires basic R skills.

1 Introduction

DNA methylation, preferentially occurring at CpG dinucleotides in mammalian genomes, correlates with cell type identity and differentiation stage[1]. Importantly, methylation states of particular CpGs can be used as powerful biomarkers for various conditions, including cancer[2–4], inflammatory diseases[5] and aging[6]. To facilitate such findings, large international consortia, including IHEC[7], DEEP[1], and BLUEPRINT[8], are generating genome-wide DNA methylation maps (or DNA methylomes) of primary tissue samples and isolated cell populations. However, DNA methylomes obtained from bulk samples are intrinsically heterogeneous, and can be additionally affected by aging, sex and other confounders. Computational methods for the integration of large-scale DNA methylation datasets, and capable of delineating such complex methylomes into biologically distinct variability components, are of paramount importance[9].

Deconvolution methods dissect methylomes of cell mixtures into their basic constituents[10]. In case reference DNA methylomes of purified cell types are available, these can be used to infer the proportions of different cell types across the samples. Multiple reference-based methods have been proposed[11–13] and are reviewed elsewhere[14] (summarized in **Supplementary Table 1**). Another class of methods allows for composition-adjusted identification of differentially methylated regions in epigenome-wide association studies (EWAS) without explicitly computing the cell type proportions[15,16]. When reference methylomes and other prior information is partially or completely absent, semi-reference-free (*BayesCCE*[17]) or fully reference-free (*RefFreeCellMix*[18], *EDec*[19], *MeDeCom*[20]) deconvolution methods can be applied (**Supplementary Table 1**). Reference-free methods are of particular benefit for poorly characterized, complex systems, where adequate reference profiles are especially hard to obtain. These tissues include for instance brain, and solid tumors. We earlier found that in a large variety of applications, reference-free deconvolution methods are only marginally different in their accuracy, and a thorough preprocessing, as well as careful feature selection are more important than the choice of the deconvolution tool[21]. Furthermore, interpretation of deconvolution results is challenging in case prior information about the investigated biological system is limited. Here, we present a comprehensive pipeline that facilitates reference-free deconvolution, starting from raw DNA methylation data down to result interpretation. Although we focus on *MeDeCom* as a representative method, the protocol is not limited to a single deconvolution method and can be used in combination with other available tools.

1.1 Development of the protocol

Reference-free deconvolution is a challenging computational task, for which several methods have been proposed, along with the tools implementing them (**Supplementary Table 1**). However, in a pilot benchmark of several published reference-free deconvolution tools, we found that their performance differences were marginal, both on fully synthetic and *in silico* mixed experimental datasets[21]. In fact, the quality and information content of the input DNA methylation matrix had a higher impact upon the accuracy, than the choice of the deconvolution tool itself. Thus, deconvolution algorithms *a priori* rely on thorough data processing and feature selection, especially if the differences between underlying components are small. Furthermore, biological interpretation of deconvolution results is often challenging, in particular for beginners with limited bioinformatic experience. Facilitating the generation of biological insights about the investigated system is similarly important as the deconvolution itself. To overcome these limitations, we developed a comprehensive, three-stage protocol, which includes critical preprocessing and interpretation steps in addition to the actual deconvolution. The protocol, schematically outlined in **Fig. 1**, consists of three main stages: (i) state-of-the-art DNA methylation data preparation, including stringent, quality-adapted CpG filtering, elimination of potential confounding factors using Independent Component Analysis (ICA) and feature selection; (ii) reference-free methylome deconvolution; (iii) interpretation of deconvolution results with a user-friendly R/Shiny-based interface, enabling generating novel biological insights.

As earlier described, data preparation is key to the overall success of deconvolution. The first stage of our protocol thus comprises quality-adapted removal of unreliable or otherwise problematic measurements using the widely used *RnBeads* software package for data handling[22,23]. Confounding factors, such as age, sex or donor genotype, can have a strong influence on the methylome, and investigators might want to adjust for those in their analyses[24,25]. Therefore, we argue that accounting for confounders, using methods such as Independent Component Analysis (ICA)[26], is crucial to obtain biologically relevant results. As the final data preparation step, a CpG subset selection determines sites that are linked to, for instance, cell type identity or any other phenotypic trait of interest.

The prepared, high-quality data matrix can be subjected to one of the deconvolution tools (**Supplementary Table 1**). As a rule, these methods decompose input DNA methylation matrix into a matrix of latent methylation components (LMCs, *T*) and a matrix of proportions (*A*). In the second stage of the protocol, we use *MeDeCom*[20], our own method based on regularized non-negative matrix factorization (NMF). To enforce the bimodality of LMCs, it regularizes the entries of *T* towards extreme values zero and one. A *MeDeCom* solution is defined by two user-specified parameters: the number of LMCs *K* (the inner dimension of *T* and *A*), and the quadratic regularization parameter λ (zero for no, and larger than one for strong regularization). Although, the generated cross validation error provides a rational criterion for parameter selection, it is often useful to consider several alternative solutions. *MeDeCom* therefore stores all results obtained on a reasonable parameter grid for subsequent in-depth exploration.

Although reference-free deconvolution is flexible with respect to the investigated system, the interpretation of deconvolution results, especially of the LMC matrix *T*, can be challenging. In addition to cell type profiles, LMCs reflect multiple drivers of biological and technical variability, including age or sex. Furthermore, validating the proportions and LMCs is not trivial, since the space of possible solutions is large and the cellular composition is typically unknown. In order to guide users, we implemented most of the interpretation functionality in the form of a specialized R/Shiny-based graphical user interface (*FactorViz*). A detailed description of the annotation and inference features implemented in *FactorViz* is given in the Outline of the Procedure section below.

1.2 Applications of the methods

Reference-free deconvolution is the method of choice for studying heterogeneity of DNA methylomes in biological systems with limited prior knowledge about their cellular composition, or in case of missing reference profiles. This includes EWAS using material from hardly-accessible or insufficiently-characterized organs and tissues, such as human brain, as well as solid tumors. Previously, we and others used this approach to understand cellular heterogeneity in placenta[27] , multiple sclerosis[28], breast cancer[19], and cholangiocarcinoma[29]. Reference-free deconvolution is particularly useful to dissect tumor heterogeneity, e.g. to study the effect of tumor-infiltrating immune cells on the tumor microenvironment[30]. Furthermore, identified LMCs can be correlated to tumor size, location, metastasis state, and mutational burden. Since tumors in general show a high degree of sample-to-sample variation, methylome deconvolution can be used to detect similarities among different types of cancers to define pan-cancer and cancer type-specific markers. If a particular cancer induces changes in the DNA methylation pattern of the tumor stroma, these changes are likely to be missed by reference-based, but not by reference-free methods.

In the original publication, after the validation on simulated data and *in-silico* cell type mixtures, *MeDeCom* was applied to a brain frontal cortex dataset, successfully separating it into neuronal and glia fractions, as well as detecting additional LMCs, which could be linked to features of Alzheimer's disease[20]. We anticipate successful application of *MeDeCom* in similar scenarios. Furthermore, although for blood-based studies reference methylomes exist and reference-based methods perform generally well, reference-free deconvolution can be useful in case of severely altered blood composition, e.g. due to an overproduction of rare cell types.

Finally, in the case of blood and other similarly well characterized tissues, *MeDeCom* can be applied in a semi-supervised fashion using *spiked-in* reference profiles. This enables easy recovery of known signatures, and allows for detection of additional unknown LMCs.

Single-cell technology is steadily improving, and cell-level DNA methylomes will become increasingly available in the near future[31,32]. Nevertheless, we expect that deconvolution of large-scale bulk tissue datasets will remain a useful complement of single cell DNA methylation profiling, which still suffers from high costs, low sample throughput and data sparsity. We envisage that both approaches can be successfully used in combination, e.g. single-cell profiling in several reference samples followed by deconvolution of bulk methylomes from large patient cohorts, where single-cell profiles can be used for interpretation of the LMCs or as pivot profiles in semi-reference-free scenarios. Finally, deconvolution of more accessible bulk methylomes can be used to integrate them with easier to obtain single-cell profiles of other omics layers, including single-cell transcriptomes and chromatin accessibility maps.

1.3 Outline of the procedure

Our protocol is divided into three main stages: (i) Data preparation, (ii) Deconvolution and (iii) Interpretation, which are described in detail below (see also **Fig. 1**).

1.3.1 Data preparation

We implemented the data preparation stage of the protocol as a new R-package (*DecompPipeline)* that integrates quality filtering, confounding factor adjustment and feature selection steps into an easy-to-use workflow (http://github.com/CompEpigen/DecompPipeline). For loading, formatting and storing DNA methylation data we recommend our recently updated *RnBeads* package*.*

***Data import*.** Genome-wide DNA methylation can be profiled by different technologies such as whole-genome bisulfite sequencing (WGBS), reduced-representation bisulfite sequencing (RRBS) or the Illumina Infinium microarrays. In this protocol we focus on microarray datasets due to their larger sample sizes that increase the efficiency of deconvolution. Nevertheless, our pipeline is similarly applicable to any other data type that provides DNA methylation calls at single CpG resolution, given at least a dozen samples are available. In addition to raw DNA methylation data, phenotypic information is required and converted into the internal *RnBeads*[22,23] data structure. The input is checked for data quality using *RnBeads'* reporting functionality.

***Quality filtering*.** *DecompPipeline* performs quality-based filtering of CpGs across the samples in several steps (**Table 1**). First, CpGs are filtered according to a coverage threshold across the samples, and overall signal intensity (microarrays) or coverage (bisulfite sequencing) outliers are removed. Missing values can either be completely discarded from the dataset or imputed[33]. We further remove sites overlapping annotated or estimated single nucleotide polymorphisms (SNPs), sites on the sex chromosomes and cross-reactive sites[34]. Infinium data should be normalized prior to downstream analysis, and further sample properties can be inferred, such as the overall immune cell content using the LUMP algorithm[35] or the epigenetic age[25].

Covariate adjustment using ICA. DNA methylomes can be affected by various sources of variability, both of biological and technical nature that might mask the signals of interest. Independent component analysis (ICA)[26] is a data-driven dimensionality reduction method that performs a matrix decomposition, dividing the experimentally observed data matrix D_{mn} into k independent signals S_{mk} mixed with the coefficients of M_{kn}:

$$D_{mn} \sim S_{mk} \times M_{kn}$$

where m and n are the number of features (methylation sites) and samples, respectively. S represents the contributions of methylation sites in different components. The weight matrix M can be linked to clinical outcomes, such as cancer type and patient survival, and confounding factors, including sex, experimental batch effects or platform biases. As the method separates the original methylation profiles into statistically independent signals, the influence of potential confounding factors on the methylation profiles can be attributed to particular CpGs, which can either be removed or the weights (rows of M) of corresponding components can be set to zero[36].

A pitfall of ICA that is specific to methylation data analysis is the smoothing of the original beta value distribution after ICA-based normalization. Therefore, a post-processing step is required in order to bring beta values into the expected range. To achieve this, reconstructed values are linearly rescaled in order to set the 1st and 99th percentiles to beta values of zero and one. Finally, in order to reduce stochasticity of ICA decomposition, we apply the consensus ICA approach[37]. ICA was run multiple times and the resulting matrices S and M were mapped and averaged between the runs. The stability of the components is estimated as the coefficient of determination (R^2) between the columns of S observed in different runs.

***Selection of informative CpG subsets*.** In order to obtain satisfactory deconvolution results, further feature selection is required, since, for instance, lowly variable CpGs do not contribute to signature recovery, but add to the computational runtime. From our experience, using prior knowledge about the underlying cell types is the best option, given such knowledge is available[11,19]. In the absence of prior knowledge about the biological system of interest, typical strategies for feature selection include selecting the most variable sites, the ones with the highest loadings on the first few principal components, or a random selection. *DecompPipeline* provides 14 options to select CpG subsets (**Table 2**[38–40]), and multiple of these options can be included in a single execution of the pipeline.

1.3.2 Performing deconvolution using MeDeCom

Reference-free deconvolution methods, such as *RefFreeCellMix*[18], *EDec*[19] or *MeDeCom*[20], estimate the matrix of latent methylation components (T) and the matrix of proportions (A) based on the DNA methylation matrix of sites selected in the previous step (D) by means of non-negative matrix factorization. We focus on *MeDeCom*, but the pipeline similarly supports *RefFreeCellMix* and *EDec*. *MeDeCom* optimizes the squared Frobenius norm of the difference between the true (measured) methylation matrix D and the matrix product of T and A (**Fig. 1**). Desired properties of the factor matrices, i.e. restriction to the [0, 1] interval (T and A) and column-sums equal to one (A), are enforced by respective constraints on their entries. Furthermore, *MeDeCom* penalizes the entries of T not equal to zero and one using quadratic regularization (maximum at entries equal to 0.5) controlled by the regularization parameter λ.

The optimization problem is solved using an alternating optimization scheme, which fixes either of *A* or *T* while fitting the other at each of its steps. Selecting suitable values for the regularization parameter (λ) and the number of latent components (*K*) is assisted by a cross-validation scheme that leaves out columns of *D*. Typically, a grid search for different values of *K* and λ is performed to determine the best number of components and regularization, respectively. In order to reduce running time substantially, we recommend activating the parallel processing options on standalone workstations, or to use a high-performance computing cluster. The resulting solutions of the deconvolution problem are stored on disk and can be used for downstream interpretation.

1.3.3 Interpretation of deconvolution results

In contrast to reference-based deconvolution, interpretation of reference-free deconvolution results is non-trivial. *MeDeCom* produces a matrix of LMCs and a matched proportion matrix, both of which need to be biologically validated and interpreted. To facilitate an interactive interpretation, we created the semi-automated visualization tool *FactorViz* (https://github.com/CompEpigen/FactorViz). *FactorViz* is an R/Shiny-based user interface with guidelines and functions for comprehensive biological inference. Initially, one of the possible *MeDeCom* solutions has to be chosen by selecting the parameters *K* and λ based on the cross-validation error. In order to investigate potential influences of covariates upon the estimated proportions and corresponding LMCs, the resulting proportion matrix is linked to technical or phenotypic traits, such as experimental batch or subject age, using association tests. Furthermore, proportions can be linked to marker gene expression values, or specific properties of the analyzed dataset such as survival time. To functionally annotate LMCs, we determine the sites that are specifically hypomethylated in a particular LMC in comparison to the median of the remaining LMCs, and treat the obtained sites as LMC-specific. Those sites are then used for GO[41] and LOLA[42] enrichment analysis in order to associate respective LMCs with functional categories, pathways and various genomic features. Finally, the matrix of LMCs can be compared with available reference cell type profiles.

1.4 Level of expertise needed to implement the method

DecompPipeline, MeDeCom, and FactorViz are R-packages and thus require some minimal prior experience with the R programming language. Basic knowledge of the Unix command line interface is recommended for data handling. To follow the steps of this protocol, one only needs a few R function calls, but the function parameters need to be tailored to the target dataset. The graphical user interface *FactorViz* presents plots, which require a minimum knowledge of DNA methylation data and matrix factorization.

1.5 Limitations

Since *MeDeCom* tests all possible combinations of the regularization parameter λ, the number of LMCs *K* and several feature selection methods, the number of basic deconvolution jobs can reach 1,000 – 10,000. Reference-free deconvolution is thus a computationally demanding task that requires high-performance computing infrastructure. When applied to larger datasets, the deconvolution can take several days to finish even on larger machines. Furthermore, the obtained LMC matrix needs to be biologically interpreted, which requires user interaction and input. A fully-automated interpretation of deconvolution results will be part of the next development steps of the protocol. Accounting for confounding factors, especially for those that might have a strong influence on the methylome, can lead to a substantially modified DNA methylation data matrix. The proposed pipeline provides diagnostic plots, but user interaction is still required to determine if the effect of a particular covariate is to be removed.

2 Materials

2.1 Hardware

We recommend to apply the proposed protocol on large systems with, e.g. 128 GB of main memory and 32 cores for a dataset of this size. For larger datasets such as bisulfite sequencing data, we recommend a transition to a high-performance compute cluster or a cloud environment, such that the pipeline can automatically distribute jobs across different machines. *MeDeCom*, *FactorViz* and *DecompPipeline* can be directly installed from GitHub on Unix-like systems, and a Docker container is available also for Windows 10 systems (https://hub.docker.com/r/mscherer/medecom).

2.2 Input data

We used publicly available data from The Cancer Genome Atlas (TCGA, https://www.cancer.gov/tcga) investigating lung adenocarcinoma (dataset TCGA-LUAD, https://portal.gdc.cancer.gov/legacy-archive/search/f) in 461 samples assayed using the Illumina 450k microarray, since lung cancer has high cellular and molecular heterogeneity[43]. The clinical metadata and the manifest file of the samples is available at https://portal.gdc.cancer.gov/projects/TCGA-LUAD and have been downloaded through the TCGA legacy archive on 2019-01-23. We used the Genomic Data Commons (GDC) data download tool (https://gdc.cancer.gov/access-data/gdc-data-transfer-tool) together with the manifest file to download the intensity data (IDAT) files and associated metadata.

3 Procedure

Installation TIMING 1 h

1. The pipeline needs R installed on your machine. If it is not yet installed, follow the instructions at https://cran.r-project.org/.

2. Invoke R on the command line and install the *devtools* package. Then, install the software packages needed for deconvolution directly from GitHub: *MeDeCom*, *DecompPipeline* and *FactorViz*, and *RnBeads* from Bioconductor.

```
install.packages(c(“devtools”,”BiocManager”))
BiocManager::install(“RnBeads”)
library(devtools)
devtools::install_github(
        c("lutsik/MeDeCom”,”CompEpigen/DecompPipeline”,"CompEpigen/FactorViz”)
)
library(DecompPipeline)
```

Data retrieval TIMING 5 h

3. Use the Genomic Data Commons (GDC) data download tool (https://gdc.cancer.gov/access-data/gdc-data-transfer-tool) to download the IDAT files listed in the manifest file and its associated metadata. This metadata also includes the mapping between each of the samples and the IDAT files.

```
gdc-client download -m gdc_manifest.2019-07-03.txt

clinical.data <- read.table(“annotation/clinical.tsv”,
                                                sep =“\ t”,
                                                header = TRUE )
idat.files <- list.files(“idat”,full.names = TRUE)
meta.files<-list.files(idat.files[1],full.names = TRUE)
untar(meta.files[3],exdir = idat.files[1])
meta.files <- untar(meta.files[3],list = TRUE)
meta.info <- read.table(file.path(idat.files[1],meta.files[5]),
                                sep =“\t”,
                                header = TRUE)
meta.info <- meta.info[match(unique(meta.info$Comment..TCGA.Barcode.),
                                meta.info$Comment..TCGA.Barcode.),]
match.meta.clin <- match(clinical.data$submitter_id,
                        substr(meta.info$Comment..TCGA.Barcode.,1,12))
anno.frame <- na.omit(data.frame(clinical.data,
                        meta.info[match.meta.clin,]))
anno.frame$barcode <- unlist(
        lapply(
                lapply(as.character(anno.frame$Array.Data.File),
                        function(x)strsplit(x,"_”)),
                function(x)paste(x[[1]][1],x[[1]][2],sep = "_”)))
anno.frame$Sentrix_ID <- unlist(
        lapply(
                lapply(as.character(anno.frame$Array.Data.File),
                        function(x)strsplit(x, "_”)),
                function(x)paste(x[[1]][1])))
anno.frame$Sentrix_Position<-unlist(
        lapply(
                lapply(as.character(anno.frame$Array.Data.File),
                        function(x)strsplit(x,"_”)),
                function(x)paste(x[[1]][2])))
write.table(anno.frame,”annotation/sample_annotation.tsv”,
        quote = FALSE, row.names = FALSE, sep = “\t”)
anno.frame <- read.table(“annotation/sample_annotation.tsv”,
        quote = FALSE, row.names = FALSE, sep = “\t”)
```

4. Copy the IDAT files into a single directory for downstream analysis.

```
lapply(idat.files,function(x){
        is.idat<-list.files(x, pattern = ".idat”, full.names = TRUE)
        file.copy(is.idat,”idat/”)
        unlink(x,recursive = TRUE)
})
```

Data import TIMING 2 h

5. *RnBeads* converts the files into a data object and performs basic quality control steps. Most notably, analysis options have to be specified for *RnBeads*, either through an XML file or through the command line. Deactivate the preprocessing, exploratory, covariate inference, export and differential methylation modules, such that RnBeads only performs data import and quality control.

```
library(RnBeads)
rnb.options(
        assembly = “hg19”,
        identifiers.column = “submitter_id”,
        import = TRUE,
        import.default.data.type = “idat.dir”,
        import.table.separator = “\t”,
        import.sex.prediction = TRUE,
        qc = TRUE,
        preprocessing = FALSE,
        exploratory = FALSE,
        inference = FALSE,
        differential = FALSE,
        export.to.bed = FALSE,
        export.to.trackhub = NULL,
        export.to.csv =  FALSE
)
```

6. Specify the input to *RnBeads*: the sample annotation sheet created at the data retrieval step, the folder in which the IDAT files are stored and a folder to which the HTML report is to be saved. Additionally, specify a temporary directory and start the *RnBeads* analysis.

```
sample.anno <- ”annotation/sample_annotation.tsv"
idat.folder <- ”idat/"
dir.report <- paste0(“report”,Sys.Date(),”/”)
temp.dir <- ”/tmp"
options(fftempdir = temp.dir)
rnb.set <- rnb.run.analysis(
        dir.reports = dir.report,
        sample.sheet = sample.anno,
        data.dir = idat.folder
)
```

7. *RnBeads* creates an interactive HTML report, specifying the steps performed and the associated results. Data should meet the quality criteria in **Table 3** to be used for downstream analysis (see also the Anticipated Results section).

Preprocessing and filtering TIMING 22 h

8. Use the *DecompPipeline* package (https://github.com/CompEpigen/DecompPipeline) for further analysis. Processing options are provided through individual function parameters. Follow a stringent filtering strategy: (i) Filter CpGs covered by less than 3 beads, and probes

that are in the 0.001 and 0.999 overall intensity quantiles (low and high intensity outliers). (ii) Remove all probes containing missing values in any of the samples. (iii) In the sequence context filtering, sites outside of CpG context, overlapping annotated SNPs, located on the sex chromosomes and potentially cross-reactive probes are discarded. Finally, upon successful filtering, apply BMIQ normalization[44] to account for the bias introduced by the two Infinium probe designs[45].

CRITICAL STEP Removing too few or too many sites might have a strong influence on the final deconvolution results. Thus, we recommend to carefully check the available options (**Table 1**) and only change the default setting in case of low-quality data.

9. Accounting for potential confounding factors is crucial in epigenomic studies and the influences of, for instance, donor sex, age, and genotype on the DNA methylation pattern are well-studied[24,25]. Use Independent Component Analysis (ICA, see Materials) to account for DNA methylation differences that are due to sex, age, race, and ethnicity.

CRITICAL STEP Confounding factor adjustment changes the overall data distribution, which might harm the overall bimodality of DNA methylation. The diagnostic plots provided by *DecompPipeline* should be carefully checked.

```
library(DecompPipeline)
data.prep <- prepare_data(RNB_SET = rnb.set,
            analysis.name = “TCGA_Deconvolution”,
            NORMALIZATION = “bmiq”,
            FILTER_BEADS = TRUE,
            MIN_N_BEADS = 3,
            FILTER_INTENSITY = TRUE,
            MIN_INT_QUANT = 0.001,
            MAX_INT_QUANT = 0.999,
            FILTER_NA = TRUE,
            FILTER_CONTEXT = TRUE,
            FILTER_SNP = TRUE,
            FILTER_SOMATIC = TRUE,
            FILTER_CROSS_REACTIVE = TRUE,
            execute.lump = TRUE,
            remove.ICA = TRUE,
            conf.fact.ICA = c(“age_at_diagnosis”,”race”,“gender”,”ethnicity"),
            ica.setting = c(“alpha.fact”= 1e-5, “save.report”=TRUE,
                                    ”ntry”= 10,”nmax”= 50,“ncores”= 10)
)
```

Selection of CpG subsets TIMING 1 min

10. Select a subset of sites to be used for deconvolution. *DecompPipeline* provides a number of options (**Table 2**) through the *prepare_CG_subsets* function. Focus on selecting the 5,000 most variable sites across the samples.

```
cg_subset <- prepare_CG_subsets(
            rnb.set = data.prep$rnb.set.filtered,
            MARKER_SELECTION = “var”,
            N_MARKERS = 5000
)
```

Methylome deconvolution TIMING 54 h

11. Perform the deconvolution experiment. Focus on MeDeCom as a robust deconvolution tool and specify a grid of values for the number of components (*K*) ranging from 2 to 15, which covers homogeneous to heterogeneous samples. Also, specify a grid for the regularization parameter (*λ*) from strong (0.01) to no regularization (0).

```
md.res <- start_medecom_analysis(
          rnb.set = data.prep$rnb.set.filtered,
          cg_groups = cg_subset,
          Ks = 2:15,
          LAMBDA_GRID = c(0,10^-(2:5)),
          factorviz.outputs = TRUE,
          analysis.name = “TCGA_LUAD”,
          cores = 15
)
```

Downstream analysis TIMING 1 h

12. Visualize and interactively explore the deconvolution results with *FactorViz* (**Supplementary Fig. 1**).

```
library(FactorViz)
startFactorViz(file.path(getwd(),”TCGA_LUAD”,”FactorViz_outputs”))
```

13. Determine the number of components and the regularization parameter from the provided list of parameters (**Supplementary Fig. 2**).

14. Associate the proportion matrix with quantitative (mutation count, fraction of genome altered, LUMP estimate, stromal score) and qualitative (sex, ethnicity, health state, copy number states) traits using correlation- and t-tests, respectively (**Supplementary Fig. 3**).

CRITICAL STEP Interpretation of deconvolution results is crucial to obtain biological insights about the investigated system. In addition to the interpretation functions provided by *FactorViz*, prior knowledge about the system can be used to validate and interpret deconvolution results.

15. Compare LMC proportions per sample to expression of epithelial, endothelial, stromal, and immune cell marker genes in lung tissue[46] (**Supplementary Text**).

16. To determine sites that are specifically hypo- and hypermethylated in an LMC, compare the methylation values in the LMC matrix for each LMC to the median of the remaining LMCs and then employ GO and LOLA enrichment analysis (**Supplementary Fig. 4**).

4 Troubleshooting

We provide troubleshooting advice in **Table 4**. For further support questions, feature requests or help, use GitHub's issue system or write a mail to the tool developers.

5 Anticipated Results

5.1 Quality control and feature selection

Deconvolution analysis requires input DNA methylation data of good technical quality, which we verified using *RnBeads'* QC module. In the example analysis, quality control probes on the Infinium array did not reveal low-quality samples to be removed. Verifiable phenotypic information matched the inferred sample properties, such as predicted sex of all subjects (**Fig. 2**). We used several criteria to select a set of high-confidence CpGs as input to *MeDeCom*. Most of the discarded sites (39.5%) were removed, because they were covered by less than three beads in any of the samples, or showed unusually high or low intensity. Further CpG filtering steps, including sequence context (SNPs, sites on the sex chromosomes, 10.5%) and removal of cross-reactive probes[34] (2.5%) eliminated further problematic sites. As a final outcome of the filtering procedure, 230,223 sites (47.4% of 485,577) passed our stringent quality criteria and were used for downstream analysis (**Fig. 2**).

5.2 Confounding factor analysis

To evaluate ICA, we applied the proposed workflow to the TCGA dataset twice: once without correcting for age, sex, race, and ethnicity, and once with the adjustment using ICA (**Fig. 3A**). ICA detected 22 components, of which two were significantly associated with sex and ethnicity, respectively (**Fig. 3B**). The overall distribution of the DNA methylation matrix was still bimodal after ICA adjustment, although there were notable peaks at methylation values zero and one, respectively. We argue that these peaks are a consequence of the linear scaling (**Fig. 3C**). After employing *MeDeCom* independently on the modified and the unadjusted DNA methylation matrix, three of the detected components were significantly linked to sex in the unadjusted (p-values: LMC1: $6x10^{-4}$, LMC4: $1.4x10^{-5}$, LMC5: $3x10^{-3}$), but only one component was mildly linked to sex in the adjusted run (LMC7, p-value: $7.8x10^{-4}$, **Fig. 3D**). Although ICA component 11 was linked to ethnicity, we could not find a similar association with LMCs. Notably, neither age nor race variables were significantly linked to any component produced by either ICA or *MeDeCom*.

5.3 Deconvolution results

The results of applying the proposed protocol to the TCGA LUAD dataset are shown in **Fig. 4**. Since we did not have prior knowledge on the expected number of underlying cell types to select, we resorted to the cross-validation procedure of *MeDeCom*. We chose 7 LMCs as the value of *K* at which the cross-validation error started to level out (**Supplementary Fig. 5A**). Similarly, we selected λ=0.001 as the regularization parameter (**Supplementary Fig. 5B**). Notably, LMC5 was particularly hypomethylated and LMC6 showed a high overall methylation level, while the remaining LMCs were rather intermediately methylated (**Supplementary Fig. 5C, D**).

We further investigated the biological implications of the detected LMCs. To this end, we found that LMC5 had substantially higher proportions in the healthy tissue samples (**Fig. 4A**). This indicated that reference-free deconvolution was able to capture the inherent methylation signatures specific to cancerous and healthy tissues. When we conducted enrichment analysis for the sites that were particularly hypomethylated in LMC5, we found that transcription factor binding sites for the Polycomb repressive complex (*SUZ12*, *EZH2*) were overrepresented. Cancers have a strong influence on the Polycomb repressive complex, which typically represses oncogenes; a process that becomes distorted when its binding sites are hypermethylated[47–49]. What is more, proportion of LMC5 in tumor tissues provided a generic estimate of tumor sample purity, i.e. degree of contamination by adjacent normal tissue. Thus, we were able to capture tumor-specific methylation signatures without conducting differential analysis between two phenotypic groups.

Next, LMC3 showed highly variable proportions across the samples and was the main driver of the overall sample clustering. LMC3 proportions were strongly correlated with the LUMP estimate (**Fig. 4B**), which predicts the overall immune cell content of a sample[35]. Furthermore, we detected enrichments of LMC3-speficic hypomethylated sites towards leukocyte (B-lymphocyte) specific transcription factor binding sites and immune response related GO terms (**Fig. 4C, D**, **Supplementary Fig. 6**). We concluded that LMC3 most likely represented tumor infiltrating immune cells. The extent of tumor infiltration might be relevant to associate cancer state to patient prognosis[50].

To determine whether the detected LMCs reflected the expression of known marker genes of lung tissue cell types, we selected *EPCAM* as an epithelial, *CLDN5* as an endothelial, *COL1A2* as a stromal, and *PTPRC* as an immune cell marker[46]. We collected gene expression data from TCGA for the samples (data processing is described in the **Supplementary Text**) and found LMC3 to be correlated to *PTPRC* expression. Furthermore, LMC1 was strongly associated with the epithelial marker expression and LMC5 with the endothelial marker *CLDN5* (**Fig. 4E**).

Many of the detected components were linked to cancer mutational status, such as overall mutation count or chromosomal gain or loss (**Supplementary Fig. 7**), or cancer stemness (**Supplementary Fig. 8**). For instance, LMC1 was inversely linked to copy number gain of chromosome 1p and 16p. We further investigated the sites that were particularly hypo- or hypermethylated in LMC4, since LMC4 showed a high proportion in a small subset of samples that clustered separately from the remaining cancer samples (**Fig. 4A**). One of these sites, cg26992600, is located 3 kb upstream of the TSS of *NKX2-8,* a gene that has potential roles in the progression of lung cancers[51] (**Supplementary Fig. 9**, **Supplementary Table 2**). Finally, in a survival analysis of LMC proportions, we found that proportions of LMC5 and LMC6 were associated with survival time (p-values: LMC5: 0.18, LMC6: 0.03, **Supplementary Fig. 10**), warranting further investigation of their biological nature, which, however, exceeded the scope of our example analysis.

Conclusions

Taken together, our methylome deconvolution protocol was able to provide novel biological insights about the cellular and intra-tumor heterogeneity of lung cancer. We expect the protocol to be of great benefit to all investigators performing DNA methylation analysis in complex and underexplored experimental systems, including bulk samples of highly heterogeneous tissues and tumors.

Funding

This work was funded in part by the German Epigenome Project (DEEP, German Science Ministry grant no. 01KU1216A), and de.NBI-epi (German Science Ministry grant no. 031L0101D). PN and TK were supported by the Luxembourg National Research Fund (C17/BM/11664971/DEMICS). PL was supported by the DKFZ Postdoctoral Fellowship and the AMPro Project of the Helmholtz Association (ZT00026).

Acknowledgements

We would like to thank the HADACA consortium (Health Data Challenge, Aussois, December 2018) for valuable input and Divanshu Gupta for thoroughly testing the proposed pipeline. We are grateful to Kersten Breuer for testing the Docker container, and to Francisco Azuaje for supporting the collaboration.

Author contributions

M.S. and P.L. implemented most of the computational procedures. P.L. previously developed and published *MeDeCom*. S.S, M.S., and P.L. implemented *FactorViz*. P.N. and T.K. implemented consensus ICA. M.S. performed the analysis of the example datasets and created all figures and tables. P.N., R.T. and V.M. provided crucial input to the analysis and interpretation, and thoroughly tested the protocol. C.P., T.L., J.W., and P.L. jointly supervised the project. M.S. and P.L. wrote the manuscript, with contributions of all co-authors. All authors read and approved the final text.

Data and code availability

The results shown here are wholly or partially based upon data generated by the TCGA Research Network: https://www.cancer.gov/tcga. The presented R packages are available from public repositories:
DecompPipeline: https://github.com/CompEpigen/DecompPipeline
MeDeCom: https://github.com/lutsik/MeDeCom
FactorViz: https://github.com/CompEpigen/FactorViz
consensusICA: https://gitlab.com/biomodlih/consica .

The pipeline behind our protocol is also implemented as a Docker container available from *DockerHub:* https://hub.docker.com/r/mscherer/medecom.

References

1. Durek, P. *et al.* Epigenomic Profiling of Human CD4+ T Cells Supports a Linear Differentiation Model and Highlights Molecular Regulators of Memory Development. *Immunity* **45**, 1148–1161 (2016).
2. Karpinski, P., Pesz, K. & Sasiadek, M. M. Pan-cancer analysis reveals presence of pronounced DNA methylation drift in CpG island methylator phenotype clusters. *Epigenomics* **9**, 1341–1352 (2017).
3. Møller, M. *et al.* Heterogeneous patterns of DNA methylation-based field effects in histologically normal prostate tissue from cancer patients. *Sci. Rep.* **7**, 40636 (2017).
4. Vidal, E. *et al.* A DNA methylation map of human cancer at single base-pair resolution. *Oncogene* **36**, 5648–5657 (2017).
5. Azuara, D. *et al.* New Methylation Biomarker Panel for Early Diagnosis of Dysplasia or Cancer in High-Risk Inflammatory Bowel Disease Patients. *Inflamm. Bowel Dis.* **24**, 2555–2564 (2018).
6. Horvath, S. & Raj, K. DNA methylation-based biomarkers and the epigenetic clock theory of ageing. *Nat. Rev. Genet.* **19**, 371–384 (2018).
7. Stunnenberg, H. G. *et al.* The International Human Epigenome Consortium: A Blueprint for Scientific Collaboration and Discovery. *Cell* **167**, 1145–1149 (2016).
8. Adams, D. *et al.* BLUEPRINT to decode the epigenetic signature written in blood. *Nat. Biotechnol.* **30**, 224–226 (2012).
9. Bock, C. Analysing and interpreting DNA methylation data. *Nat. Rev. Genet.* **13**, 705–719 (2012).
10. Teschendorff, A. E. & Relton, C. L. Statistical and integrative system-level analysis of DNA methylation data. *Nat. Rev. Genet.* **19**, 129-147 (2017).
11. Houseman, E. A. *et al.* DNA methylation arrays as surrogate measures of cell mixture distribution. *BMC Bioinformatics* **13**, 86 (2012).
12. Teschendorff, A. E., Breeze, C. E., Zheng, S. C. & Beck, S. A comparison of reference-based algorithms for correcting cell-type heterogeneity in Epigenome-Wide Association Studies. *BMC Bioinformatics* **18**, 105 (2017).
13. Chakravarthy, A. *et al.* Pan-cancer deconvolution of tumour composition using DNA methylation. *Nat. Commun.* **9**, 3220 (2018).
14. Kaushal, A. *et al.* Comparison of different cell type correction methods for genome-scale epigenetics studies. *BMC Bioinformatics* **18**, 216 (2017).
15. Zou, J., Lippert, C., Heckerman, D., Aryee, M. & Listgarten, J. Epigenome-wide association studies without the need for cell-type composition. *Nat. Methods* **11**, 309–311 (2014).
16. Rahmani, E. *et al.* Sparse PCA corrects for cell type heterogeneity in epigenome-wide association studies. *Nat. Methods* **13**, 443–445 (2016).
17. Rahmani, E. *et al.* BayesCCE: a Bayesian framework for estimating cell-type composition from DNA methylation without the need for methylation reference. *Genome Biol.* **19**, 1–18 (2018).
18. Houseman, E. A. *et al.* Reference-free deconvolution of DNA methylation data and mediation by cell composition effects. *BMC Bioinformatics* **17**, 259 (2016).
19. Onuchic, V. *et al.* Epigenomic Deconvolution of Breast Tumors Reveals Metabolic Coupling between Constituent Cell Types. *Cell Rep.* **17**, 2075–2086 (2016).
20. Lutsik, P. *et al.* MeDeCom: discovery and quantification of latent components of

heterogeneous methylomes. *Genome Biol.* **18**, 55 (2017).

21. Decamps, C. *et al.* Guidelines for cell-type heterogeneity quantification based on a comparative analysis of reference-free DNA methylation deconvolution software. Preprint at https://www.biorxiv.org/content/10.1101/698050v1 (2019).
22. Assenov, Y. *et al.* Comprehensive analysis of DNA methylation data with RnBeads. *Nat. Methods* **11**, 1138–1140 (2014).
23. Müller, F. *et al.* RnBeads 2.0: comprehensive analysis of DNA methylation data. *Genome Biol.* **20**, 55 (2019).
24. Heyn, H. *et al.* Distinct DNA methylomes of newborns and centenarians. *Proc. Natl. Acad. Sci.* **109**, 10522–10527 (2012).
25. Horvath, S. DNA methylation age of human tissues and cell types. *Genome Biol.* **14**, R115 (2013).
26. Sompairac, N. *et al.* Independent Component Analysis for Unraveling the Complexity of Cancer Omics Datasets. *Int. J. Mol. Sci.* **20**, 4414 (2019).
27. Everson, T. M. *et al.* Cadmium-associated differential methylation throughout the placental genome: Epigenome-wide association study of two U.S. birth cohorts. *Environ. Health Perspect.* **126**, 1–13 (2018).
28. Carlström, K. E. *et al.* Therapeutic efficacy of dimethyl fumarate in relapsing-remitting multiple sclerosis associates with ROS pathway in monocytes. *Nat. Commun.* **10**, 3081 (2019).
29. Goeppert, B. *et al.* Integrative Analysis Defines Distinct Prognostic Subgroups of Intrahepatic Cholangiocarcinoma. *Hepatology* **69**, 2091–2106 (2019).
30. Man, Y. G. *et al.* Tumor-infiltrating immune cells promoting tumor invasion and metastasis: Existing theories. *J. Cancer* **4**, 84–95 (2013).
31. Luo, C. *et al.* Single-cell methylomes identify neuronal subtypes and regulatory elements in mammalian cortex. *Science.* **357**, 600–604 (2017).
32. Mulqueen, R. M. *et al.* Highly scalable generation of DNA methylation profiles in single cells. *Nat. Biotechnol.* **36**, 428–431 (2018).
33. Troyanskaya, O. *et al.* Missing value estimation methods for DNA microarrays. *Bioinformatics* **17**, 520–525 (2001).
34. Chen, Y. A. *et al.* Discovery of cross-reactive probes and polymorphic CpGs in the Illumina Infinium HumanMethylation450 microarray. *Epigenetics* **8**, 203–209 (2013).
35. Aran, D., Sirota, M. & Butte, A. J. Systematic pan-cancer analysis of tumour purity. *Nat. Commun.* **6**, 8971 (2015).
36. Dirkse, A. *et al.* Stem cell-associated heterogeneity in Glioblastoma results from intrinsic tumor plasticity shaped by the microenvironment. *Nat. Commun.* **10**, 1787 (2019).
37. Nazarov, P. V *et al.* Deconvolution of transcriptomes and miRNomes by independent component analysis provides insights into biological processes and clinical outcomes of melanoma patients. *BMC Med. Genomics* **12**, 132 (2019).
38. Ritchie, M. E. *et al.* limma powers differential expression analyses for RNA-sequencing and microarray studies. *Nucleic Acids Res.* **43**, e47 (2015).
39. Jaffe, A. E. & Irizarry, R. A. Accounting for cellular heterogeneity is critical in epigenome-wide association studies. *Genome Biol.* **15**, R31 (2014).
40. Prive, F., Aschard, H., Ziyatdinov, A. & Blum, M. G. B. Efficient analysis of large-scale genome-wide data with two R packages: Bigstatsr and bigsnpr. *Bioinformatics* **34**, 2781–2787 (2018).

41. Falcon, S. & Gentleman, R. Using GOstats to test gene lists for GO term association. *Bioinformatics* **23**, 257–258 (2007).
42. Sheffield, N. & Bock, C. LOLA:Enrichment analysis for genomic region sets and regulatory elements in R and Bioconductor. *Bioinformatics* **32**, 587–589 (2016).
43. Testa, U., Castelli, G. & Pelosi, E. Lung cancers: Molecular characterization, clonal heterogeneity and evolution, and cancer stem cells. *Cancers (Basel).* **10**, 1–81 (2018).
44. Teschendorff, A. E. *et al.* A beta-mixture quantile normalization method for correcting probe design bias in Illumina Infinium 450 k DNA methylation data. *Bioinformatics* **29**, 189–196 (2013).
45. Bibikova, M. *et al.* High density DNA methylation array with single CpG site resolution. *Genomics* **98**, 288–295 (2011).
46. Sit, R. V, Chang, S., Conley, S. D., Mori, Y. & Seita, J. A molecular cell atlas of the human lung from single cell RNA sequencing. Preprint at https://www.biorxiv.org/content/10.1101/742320v1 (2019).
47. Hahn, M. A. *et al.* Methylation of Polycomb target genes in intestinal cancer is mediated by inflammation. *Cancer Res.* **68**, 10280 (2008).
48. Varambally, S. *et al.* The polycomb group protein EZH2 is involved in progression of prostate cancer. *Nature* **419**, 624–9 (2002).
49. Cai, Y. *et al.* Epigenetic alterations to Polycomb targets precede malignant transition in a mouse model of breast cancer. *Sci. Rep.* **8**, 1–12 (2018).
50. Ward, M. J. *et al.* Tumour-infiltrating lymphocytes predict for outcome in HPV-positive oropharyngeal cancer. *Br. J. Cancer* **110**, 489–500 (2014).
51. Harris, T. *et al.* Both gene amplification and allelic loss occur at 14q13.3 in lung cancer. *Clin. Cancer Res.* **17**, 690–699 (2011).
52. Benajmini, Y. & Hochberg, Y. Controlling the False Discovery Rate: A Practical and Powerful Approach to Multiple Testing. *J. R. Stat. Soc. Ser. B* **57**, 289–300 (1995).

Figure legends

Figure 1: Overview of the proposed deconvolution protocol. DNA methylation data can be used from any technology yielding single CpG methylation calls. Methylation data is first processed using *DecompPipeline*, which includes data import, preprocessing, accounting for confounders and feature selection. *MeDeCom* can be used to perform deconvolution of the input methylation matrix (dimension *m* CpGs x *n* samples) into the latent methylation components (LMCs) and the proportions matrix (dimension *K* LMCs x *n* samples), while the protocol is also applicable to different deconvolution tools. The obtained matrices are then validated and interpreted using the R/Shiny visualization tool *FactorViz*.

Figure 2: Quality control of TCGA data. **A** Boxplot for hybridization control probes for the green and the red channel, respectively. **B** Sex prediction based on the intensities of the probes on the sex chromosomes. A logistic regression classifier was employed to differentiate between female and male samples. **C** Outline of the CpG filtering procedure. The sites on the

450k array are filtered according to quality scores (coverage, overall intensity), genomic sequence context (SNPs, sex chromosomes), and cross-reactive sites are discarded.

Figure 3: Evaluation of ICA on the TCGA LUAD dataset. **A** Overview of the ICA procedure. Components linked to confounding factors (here sex, age, ethnicity or race) are removed from the contribution matrix and an adjusted DNA methylation matrix is constructed. **B** Associations between the confounding factor sex and ethnicity with the entries of the proportion matrix *M* produced by ICA. **C** Beta-value distributions of the transformed (*D**) and the untransformed (*D*) DNA methylation matrices. **D** Associations between LMC proportions and qualitative phenotypic traits. The color represents the absolute difference of the mean LMC proportions in the different groups defined by the phenotypic traits and significant p-values according to a t-test are indicated by a bold border.

Figure 4: Interpreting *MeDeCom* results with *FactorViz*. **A** Proportion heatmap of LMCs in the different samples. We selected K=7 LMCs and set λ=0.001. The samples were hierarchically clustered according to the Euclidean distance between the proportions using complete linkage. We annotated samples using disease status and with the sample-specific LUMP estimate. **B** Associations between the phenotypic traits and LMC proportions. For quantitative traits, the correlations are shown as ellipses that are directed to the upper right for positive and to the lower right for negative correlations, respectively. For qualitative traits, the absolute difference of the proportions in the two groups (e.g. female vs. male) is shown. P-values (correlation test for quantitative and t-test for categorical variables) less than 0.01 are indicated by bold borders. LOLA[42] (**C**) and GO[41] (**D**) enrichment analysis of the LMC-specific hypomethylated sites for LMCs 1, 3 and 5. No significant GO enrichment was found for LMC 1 and 5. Sites were defined as LMC-specific hypomethylated if the difference between the LMC value and the median of all other LMCs was lower than 0.5. P-values have been adjusted for multiple testing with the Benjamini-Hochberg method[52]. **E** Scatterplots between LMC proportions per sample and known marker gene expression of different lung cell types. The gene expression was measured using counts per million (CPM).

Table 1: Quality filtering steps and default parameters in *DecompPipeline.*

STEP	SITES FILTERED	DEFAULT PARAMETERS
BEAD FILTERING	Covered by less than *MIN_N_BEADS* beads in any of the samples	*MIN_N_BEADS*=3
INTENSITY FILTERING	High or low coverage outliers according to the overall intensity quantiles specified via *MIN_INT_QUANT* and *MAX_INT_QUANT*	*MIN_INT_QUANT*=0.01 *MAX_INT_QUANT*=0.99
MISSING VALUE FILTERING	Containing a missing value in any of the samples	*FILTER_NA*=TRUE
SNP FILTERING	Annotated to SNPs according to the *dbSNP*[33] database	*FILTER_SNP*=TRUE
SOMATIC SITE FILTERING	Located on the sex chromosomes	*FILTER_SOMATIC*=TRUE
CROSS-REACTIVE FILTERING	Reported to be cross reactive[34]	FILTER_CROSS_REACTIVE =TRUE

Table 2: CpG selection options available in *DecompPipeline.*

CPG SELECTION METHOD	CPG SUBSET SELECTED	DETAILS
ALL	All that fulfill the quality criteria	
PHENO	Differentially methylated according to specified phenotypic groups using the *limma* method	Ritchie *et al.*[38]
HOUSEMAN2012	50,000 listed as cell-type specific in the reference-based deconvolution method by Houseman *et al.*	Houseman *et al.*[11]
HOUSEMAN2014	According to the *RefFreeEWAS* method	Houseman *et al.*[18]
JAFFE2014	Cell-type specific in Jaffe *et al.*	Jaffe *et al.*[39]
ROWFSTAT	Linked to given reference profiles using the F-statistics	Requires reference profiles
RANDOM	Random subset	
PCA	Highest loadings on the first *N_PRIN_COMP* principal components	Default *N_PRIN_COMP=10*
VAR	Most variable across the samples	
HYBRID	Half as most variable, half randomly	
RANGE	Largest range across the samples	
PCADAPT	Principal Component Analysis implemented in the *bigstatsr* R-package	Privé *et al.*[40]
EDEC_STAGE0	According to Stage 0 of the *EDec* approach.	Requires reference profiles Onuchic *et al.*[19]
CUSTOM	User-specified list	

Table 3: Quality criteria for different quality control steps

STEP	QUALITY CRITERION
CONTROL PROBES	All background control probes should show background intensity values in the range of 1,000-2,000. The low, medium and high control probes should show a substantially higher signal intensity in the range >10,000. Samples with high background intensity or low signal intensity should be discarded from the analysis.
SNP METHYLATION	The Illumina BeadArrays contain a few highly variable SNP probes, which should have methylation values close to 0, 0.5 and 1. In a genetically matched setup, samples from a similar genotype (e.g. the same family) should cluster together using the methylation values of these SNP probes. By this approach, potential sample mix-ups can be detected.
SEX PREDICTION	Patient sex can be reliably predicted from the signal intensities of the sites on the sex chromosomes. *RnBeads* trained a robust logistic regression classifier on a large training dataset. If predicted sex does not match the annotated sex, this might indicate a sample mix-up.

Table 4: Troubleshooting for the individual steps of the reference-free deconvolution protocol.

STEP	PROBLEM	POSSIBLE REASON	SOLUTION
2	MeDeCom is not installed properly.	Package dependencies are missing	Use a Unix-like operating system.
6	RnBeads stops unexpectedly.	The report directory already exists.	Specify a path to a non-existing directory.
6	RnBeads throws an error message.	Package dependencies are not properly configured.	Check the RnBeads website (http://rnbeads.org) for potential solutions.
8	All sites are removed during filtering.	The provided quality criteria were too stringent.	Provide less stringent quality criteria. Particularly, MAX_INT_QUANT, MIN_INT_QUANT and MIN_N_BEADS have a strong influence.
9	DecompPipeline stops during confounding factor adjustment.	The system runs out of memory.	Reduce the number of components tested (nmax), the number of cores used (ncores) or the number of independent ICA runs (ntry).
11	MeDeCom does not finish properly.	The system runs out of memory.	Check the log-files in the project directory and potentially get a larger machine to perform deconvolution.
12	FactorViz does not show any of the plots described here.	MeDeCom has not finished properly.	Check the log-files in the project directory.

Figure 1

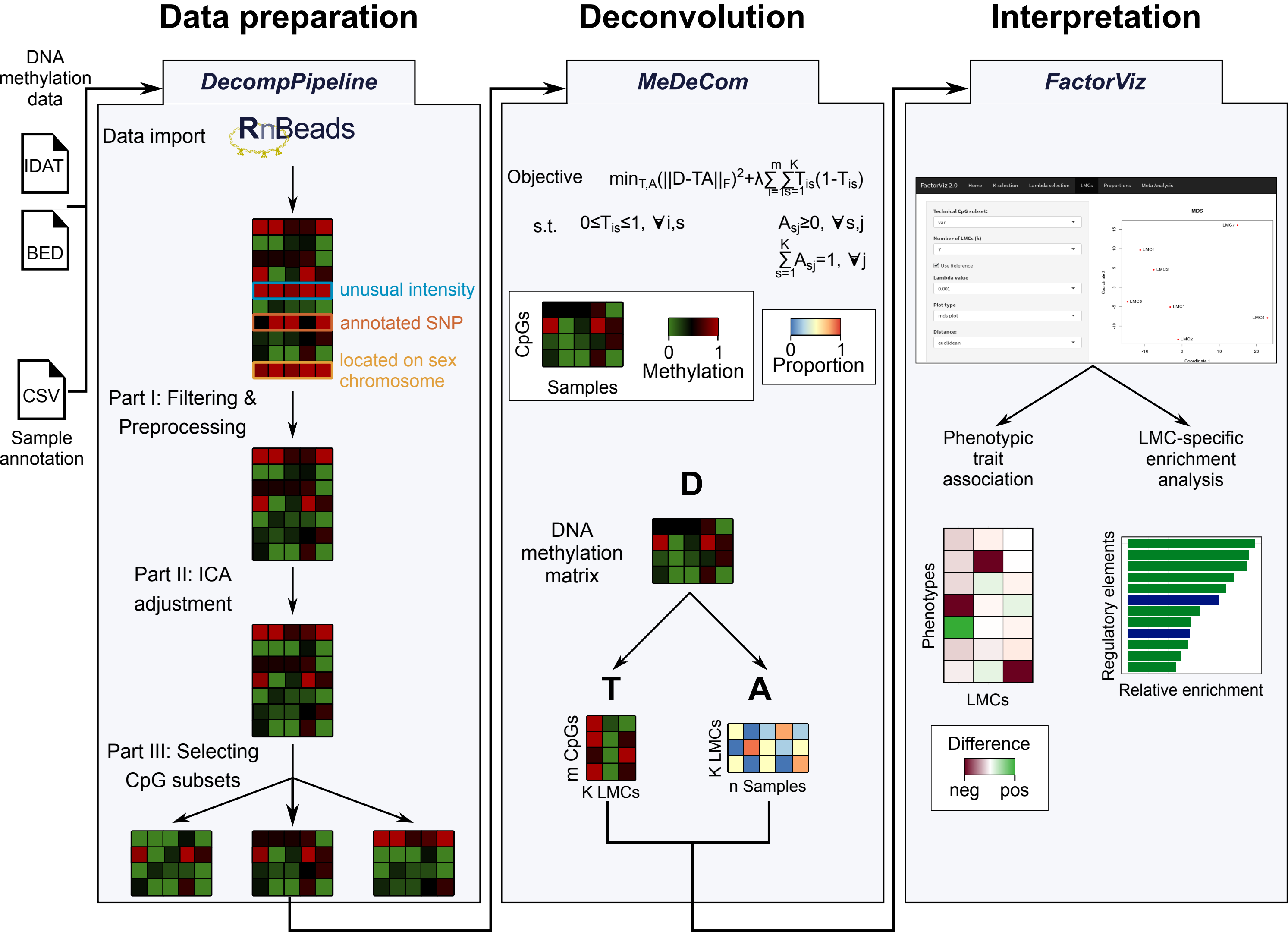

Objective $\min_{T,A}(||D-TA||_F)^2+\lambda\sum_{i=1}^{m}\sum_{s=1}^{K}T_{is}(1-T_{is})$

s.t. $0\le T_{is}\le 1,\ \forall i,s$ $\quad A_{sj}\ge 0,\ \forall s,j$ $\quad \sum_{s=1}^{K}A_{sj}=1,\ \forall j$

FactorViz 2.0 Home K selection Lambda selection LMCs Proportions Meta Analysis

Technical CpG subset: var

Number of LMCs (k): 7

☑ Use Reference

Lambda value: 0.001

Plot type: mds plot

Distance: euclidean

Figure 2

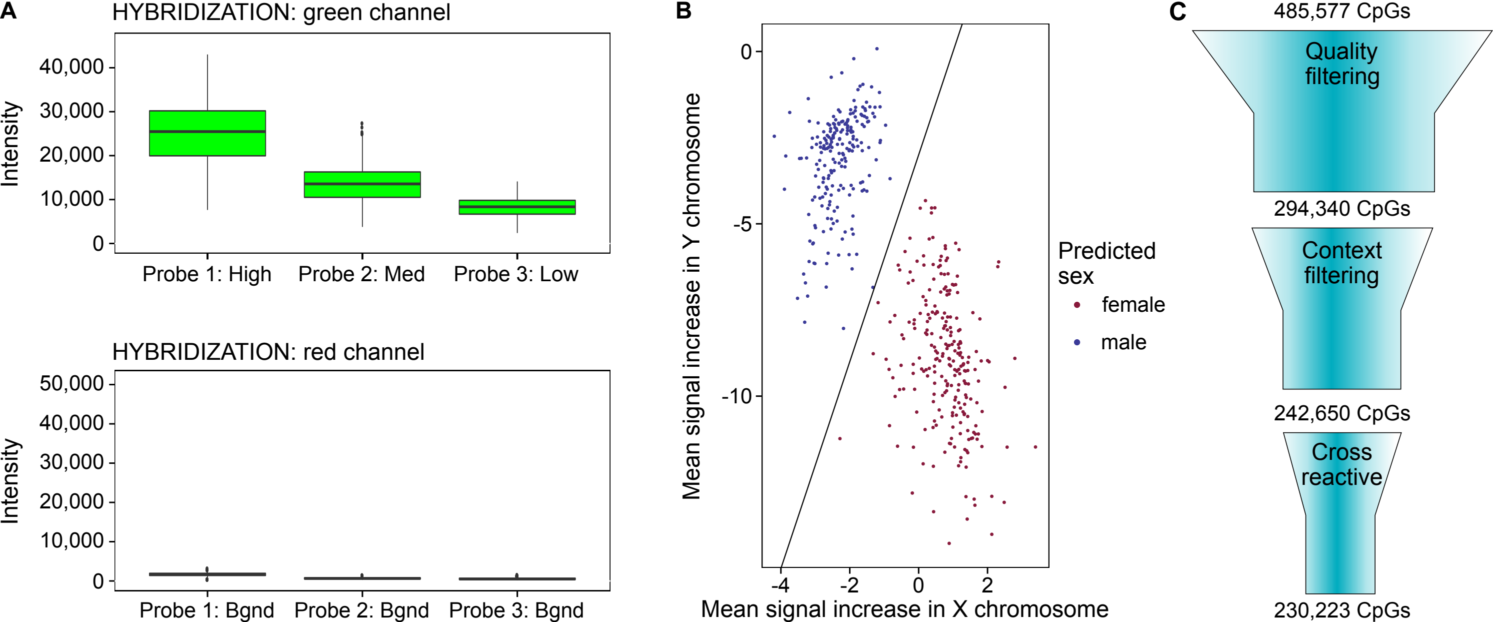
A
HYBRIDIZATION: green channel
Intensity
40,000
30,000
20,000
10,000
0
Probe 1: High
Probe 2: Med
Probe 3: Low
HYBRIDIZATION: red channel
Intensity
50,000
40,000
30,000
20,000
10,000
0
Probe 1: Bgnd
Probe 2: Bgnd
Probe 3: Bgnd
B
Mean signal increase in Y chromosome
0
-5
-10
-4
-2
0
2
Mean signal increase in X chromosome
Predicted sex
● female
● male
C
485,577 CpGs
Quality filtering
294,340 CpGs
Context filtering
242,650 CpGs
Cross reactive
230,223 CpGs

Figure 3

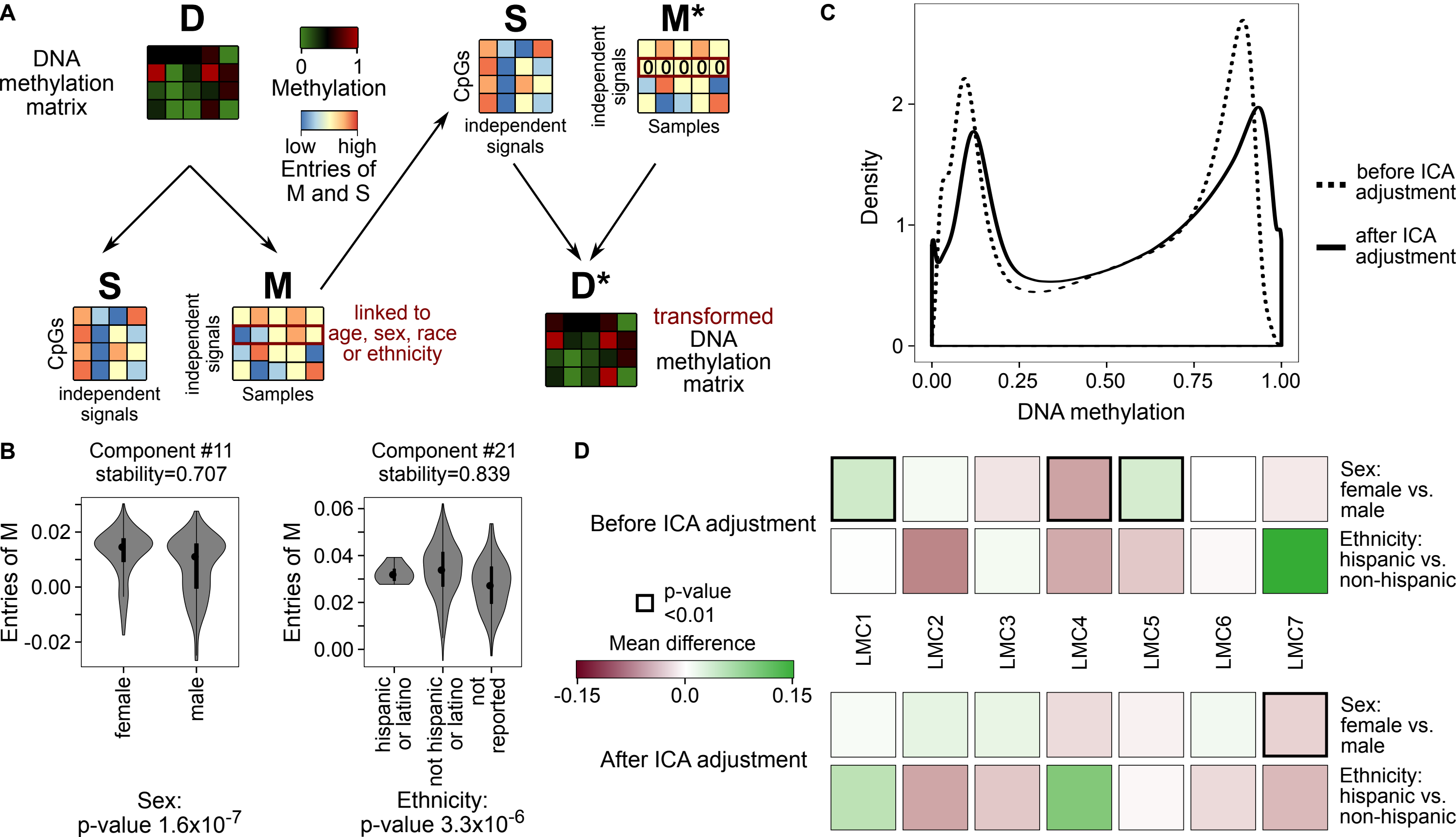
A
DNA methylation matrix
D
0
1
Methylation
low
high
Entries of M and S
S
CpGs
independent signals
M*
independent signals
0 0 0 0 0
Samples
S
CpGs
independent signals
M
independent signals
Samples
linked to age, sex, race or ethnicity
D*
transformed DNA methylation matrix
C
Density
0
1
2
0.00
0.25
0.50
0.75
1.00
DNA methylation
before ICA adjustment
after ICA adjustment
B
Component #11
stability=0.707
Entries of M
0.02
0.00
-0.02
female
male
Sex:
p-value 1.6x10^-7
Component #21
stability=0.839
Entries of M
0.06
0.04
0.02
0.00
hispanic or latino
not hispanic or latino
not reported
Ethnicity:
p-value 3.3x10^-6
D
Before ICA adjustment
p-value <0.01
Mean difference
-0.15
0.0
0.15
After ICA adjustment
LMC1
LMC2
LMC3
LMC4
LMC5
LMC6
LMC7
Sex: female vs. male
Ethnicity: hispanic vs. non-hispanic
Sex: female vs. male
Ethnicity: hispanic vs. non-hispanic

Figure 4

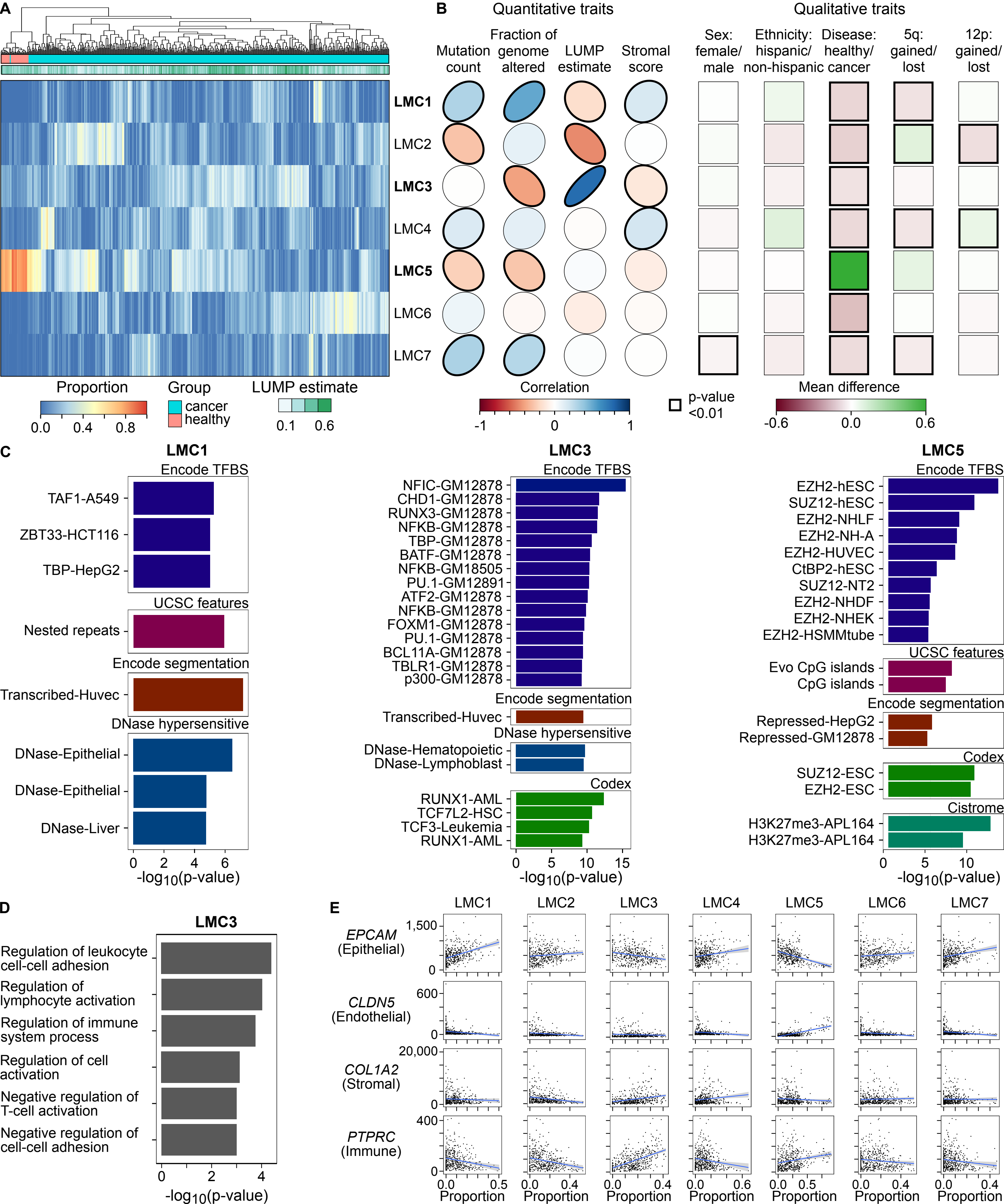

A
Proportion
0.0
0.4
0.8
Group
cancer
healthy
LUMP estimate
0.1
0.6
LMC1
LMC2
LMC3
LMC4
LMC5
LMC6
LMC7
B
Quantitative traits
Mutation count
Fraction of genome altered
LUMP estimate
Stromal score
Qualitative traits
Sex: female/ male
Ethnicity: hispanic/ non-hispanic
Disease: healthy/ cancer
5q: gained/ lost
12p: gained/ lost
Correlation
-1
0
1
p-value <0.01
Mean difference
-0.6
0.0
0.6
C
LMC1
Encode TFBS
TAF1-A549
ZBT33-HCT116
TBP-HepG2
UCSC features
Nested repeats
Encode segmentation
Transcribed-Huvec
DNase hypersensitive
DNase-Epithelial
DNase-Epithelial
DNase-Liver
0
2
4
6
-log10(p-value)
LMC3
Encode TFBS
NFIC-GM12878
CHD1-GM12878
RUNX3-GM12878
NFKB-GM12878
TBP-GM12878
BATF-GM12878
NFKB-GM18505
PU.1-GM12891
ATF2-GM12878
NFKB-GM12878
FOXM1-GM12878
PU.1-GM12878
BCL11A-GM12878
TBLR1-GM12878
p300-GM12878
Encode segmentation
Transcribed-Huvec
DNase hypersensitive
DNase-Hematopoietic
DNase-Lymphoblast
Codex
RUNX1-AML
TCF7L2-HSC
TCF3-Leukemia
RUNX1-AML
0
5
10
15
-log10(p-value)
LMC5
Encode TFBS
EZH2-hESC
SUZ12-hESC
EZH2-NHLF
EZH2-NH-A
EZH2-HUVEC
CtBP2-hESC
SUZ12-NT2
EZH2-NHDF
EZH2-NHEK
EZH2-HSMMtube
UCSC features
Evo CpG islands
CpG islands
Encode segmentation
Repressed-HepG2
Repressed-GM12878
Codex
SUZ12-ESC
EZH2-ESC
Cistrome
H3K27me3-APL164
H3K27me3-APL164
0
5
10
-log10(p-value)
D
LMC3
Regulation of leukocyte cell-cell adhesion
Regulation of lymphocyte activation
Regulation of immune system process
Regulation of cell activation
Negative regulation of T-cell activation
Negative regulation of cell-cell adhesion
0
2
4
-log10(p-value)
E
LMC1
LMC2
LMC3
LMC4
LMC5
LMC6
LMC7
EPCAM (Epithelial)
1,500
0
CLDN5 (Endothelial)
600
0
COL1A2 (Stromal)
20,000
0
PTPRC (Immune)
400
0
0.0
0.5
0.0
0.4
0.0
0.4
0.0
0.6
0.0
0.5
0.0
0.4
0.0
0.4
Proportion
Proportion
Proportion
Proportion
Proportion
Proportion
Proportion